УДК 539.125.523.348+539.126.4

SUBTHRESHOLD ρ AND J/ψ PRODUCTION ON NUCLEI (MONTE — CARLO SIMULATION)

M.Penţia[1], D.Pop[1], N.Ghiordănescu[2], A.G.Litvinenko, A.I.Malakhov, G.L.Melkumov, P.I.Zarubin, V.K.Bondarev[3]

The vector meson production, below the nucleon-nucleon kinematical limit, was studied by extending the general cross section description for stable particle subthreshold production. The final state particle distributions due to ρ and J/ψ meson production and subsequent decay were investigated by Monte — Carlo simulation and phase space integration.

The investigation has been performed at the Laboratory of High Energies, JINR.

Подпороговое образование резонансов ρ и J/ψ на ядрах (Моделирование методом Монте — Карло)

М.Пенция и др.

Проанализирован процесс рождения векторных мезонов за кинематическим пределом нуклон-нуклонных соударений с помощью обобщения сечения рождения стабильных кумулятивных частиц. Распределения частиц от распада резонансов ρ и J/ψ исследовались методом Монте — Карло и интегрированием по фазовому пространству.

Работа выполнена в Лаборатории высоких энергий ОИЯИ.

1. Subthreshold Particle Production

A lot of experimental and theoretical works [1—6] on high momentum transfer relativistic nuclear reactions are studying the particle production below the kinematical limit of the nucleon-nucleon interaction. Generally, in an inclusive nucleus-nucleus interaction:

$$A + B \to 0 + \ldots + X \qquad (1)$$

the threshold for the 0 denoted particle production can be related to the x_A and x_B scale variable [4]. It represents the fraction of the p_A and p_B 4-momentum of the target and beam particle that could produce

[1]Institute for Nuclear Physics and Engineering, Bucharest, Romania
[2]Bucharest University, Romania
[3]St. Petersburg University, Russia

the 0 particle with a given p_0, for the minimum of the squared total CM energy of the interacting constituents:

$$s = (x_A \cdot p_A + x_B \cdot p_B)^2. \tag{2}$$

It means the experimental particle spectra can be described [6] by the minimum value $s_{\min}$. It is expressed by the 4-momentum conservation law and condition of minimum:

$$\begin{cases} (x_A \cdot p_A + x_B \cdot P_B - p_0)^2 = M_X^2 \\ \dfrac{ds}{dx} = 0, \end{cases} \tag{3}$$

which give the x_A and x_B values along with the $s_{\min}$ one.

If x_A and x_B are expressed in nucleon mass fraction:

$$X_A = \frac{x_A \cdot m_A}{m_N}, \quad X_B = \frac{x_B \cdot m_B}{m_N}, \tag{4}$$

the new variables, when they are $X_A > 1$ or $X_B > 1$, formally define the subthreshold production processes.

The differential cross section for the general process (1) is expressed by the square of the matrix element $|\mathfrak{M}|^2$, by the primary particles flux density Φ and the Lorentz invariant phase space element dLips [7]:

$$d\sigma = \frac{|\mathfrak{M}|^2}{\Phi} \mathrm{dLips} =$$

$$= \frac{|\mathfrak{M}|^2}{4\sqrt{(p_A p_B)^2 - m_A^2 m_B^2}} (2\varphi)^2 \sigma^4 \left[p_A + p_B - (p_0 + \ldots + p_X)\right] \times \tag{5}$$

$$\times \frac{d^3 p_0}{(2\pi)^3 2E_0} \prod_x \frac{d^3 p_X}{(2\pi)^3 2E_X}.$$

But, for given m_A, m_B, p_A and p_B we can write:

$$d\sigma_0 = \frac{d^3 p_0}{2E_0} f(m_0, \vec{p}_0), \tag{6}$$

and the $f(m_0, \vec{p}_0)$ could be taken from the experimental data on stable particle subthreshold production [6]:

$$f(m_0, \vec{p}_0) = K \exp\left[-\frac{\sqrt{s_{\min}}}{\langle s_{\min}^{1/2}\rangle}\right]\left[0.9 \exp(-2.7|\vec{p}_0|^2 \sin^2\theta_0) + 0.1\right]. \quad (7)$$

We extended this general behaviour of the cross section (6) to unstable (resonance) particle production.

2. Particle Production and Decay Rate

Production rate of an unstable 0 particle in inclusive reaction (1) depends, besides the cross section, also on the overall decay rate term. As the process looks like:

$$\begin{aligned} x_A \cdot m_A + x_B \cdot m_B &\to m_0 + M_X, \\ &\;\;\vdots \\ &\;\;\vdots \\ &\;\;\vdots \\ &\;\;\downarrow \\ &\;\;\vdots \\ &\;\;\vdots \\ &\;\;\vdots \\ &\;\;\to m_1 + m_2 \end{aligned} \quad (8)$$

then the production rate is:

$$\frac{dN_0}{dt} = \Phi_B \sigma_0 N_A - \Gamma N_0, \quad (9)$$

where: Φ_B is the flux density of the beam particles; σ_0, the inclusive cross section for the 0 particle production; N_A, the number of the A target particles; Γ, the decay probability in time unit, for the 0 particle. After a proper integration, the time asymptotically differential distribution of the 0 particle will be:

$$dN_0 = \frac{\Phi_B N_A}{\Gamma} d\sigma_0 . \quad (10)$$

The decay rate of the 0 particles into the final state element $d\vec{p}_1 \cdot d\vec{p}_2$ can be written by multiplying this dN_0 particle number with the transition probability [7]:

$$dR_{12} = \frac{1}{2E_0} |\mathfrak{M}_{0 \to 1+2}|^2 (2\pi)^4 \sigma^4(p_0 - p_1 - p_2) \frac{d\vec{p}_1}{(2\pi)^3 2E_1} \frac{d\vec{p}_2}{(2\pi)^3 2E_2} dN_0, \quad (11)$$

$d\sigma_0$ in (10) is the differential cross section (6) and Γ is the decay probability in time unit to all possible momenta $\vec{p}_1$ and $\vec{p}_2$:

$$\Gamma = \frac{1}{2E_0} |\mathfrak{M}_{0 \to 1+2}|^2 (2\pi)^4 \int \sigma^4(p_0 - p_1 - p_2) \frac{d\vec{p}_1}{(2\pi)^3 2E_1} \frac{d\vec{p}_2}{(2\pi)^3 2E_2} . \quad (12)$$

For unpolarized particle production, the $|\mathfrak{M}_{0\to 1+2}|^2$ are constant, and the integral in (12) is the two-particle phase space one [8]:

$$\int \sigma^4(p_0 - p_1 - p_2) \frac{d\vec{p}_1}{(2\pi)^3 2E_1} \frac{d\vec{p}_2}{(2\pi)^3 2E_2} = \frac{|\vec{p}_1^*|\pi}{m_0}, \tag{13}$$

where: $|\vec{p}_1^*| = \sqrt{E_1^{*2} - m_1^2}$; $E_1^* = (m_0^2 + m_1^2 - m_2^2)/(2m_0)$.

If the m_0 mass distribution is taken as a Breit—Winger one:

$$\frac{1}{N_0}\frac{dN_0}{dm_0} = \frac{\Gamma/(2\pi)}{(m_0 - m_R)^2 + (\Gamma/2)^2}, \tag{14}$$

then the complete differential distribution of the decay rate into the final state element $d\vec{p}_1 \cdot d\vec{p}_2$ is given by (11), accounting also the (10), (6), (12), (13) and (14):

$$dR_{12} = \Phi_B N_A \frac{m_0}{|\vec{p}_1^*|\pi} \sigma^4(p_0 - p_1 - p_2) \frac{1}{N_0}\frac{dN_0}{dm_0} dm_0 \times$$

$$\times f(m_0, \vec{p}_0) \frac{d\vec{p}_0}{2E_0} \frac{d\vec{p}_1}{2E_1} \frac{d\vec{p}_2}{2E_2}. \tag{15}$$

3. The Final State Particle Distributions Due to ρ and J/ψ Subthreshold Production and Decay

The final state particle distribution, due to unstable particle production and decay, gives the necessary elements to design and arrange the experimental work. They show the spectral characteristics due to both kinematics of the process and its dynamics. So, it is possible to correlate the action of different detection elements, to organize an efficient trigger system and to optimize the detector configuration for a given physical process study.

Any one of the possible distributions is done by integrating the dR_{12} element (15) over all the variables, except the one specifying the distribution itself, which is taken in constant steps on every surface, corresponding to constant values of this variable. The multiple integration, in this work, was carried out by Monte — Carlo method [9].

The simulated physical processes are an 8.9 GeV/c proton-nucleus interaction, followed by a 0 (ρ and J/ψ) particle production and decay.

The cross section is taken from the stable meson subthreshold production [6] and is extended to this vector meson production. We considered the two particle final states (pions from ρ meson decay and electrons from J/ψ meson decay) for integration over their phase space and sought the characteristic distributions.

The $\vec{p}_0$ momentum is taken as a constant vector, as long as m_0 takes Breit — Wigner distributed values. The final particle momentum vectors $\vec{p}_1$ and $\vec{p}_2$, are generated as two constant module opposite vectors $|\vec{p}^*|$, isotropically distributed in the CM system of the decaying particle, followed by a general Lorentz transformation to the laboratory system.

The most interesting distributions are presented in the Figures 1—11. Every one is based on 100,000 generated events. The lines on all the graphics are drawn by a spline fit procedure. In the next, we will analyze the ρ and J/ψ distributions. The main differences are due to the fact that the resonance width is large for ρ meson (Γ = 153 MeV) and small for J/ψ meson (Γ = 0.00472 MeV).

— The cross section changes strongly on the ρ mass interval, but on the J/ψ mass interval it is practically constant. Consequently, the two-pion *effective mass distribution*, from the ρ meson decay, (the same with its mass distribution), shows a strong cross section dependence especially in the low mass part (Fig.1), while the high mass part shows a Breit — Wigner behaviour.

By contrary, the two-electron effective mass distribution from the J/ψ decay has not any cross section influence, neither on the J/ψ mass nor on its momentum and angle values. It is the same with the Breit — Wigner distribution.

— The one-particle *energy distributions* for

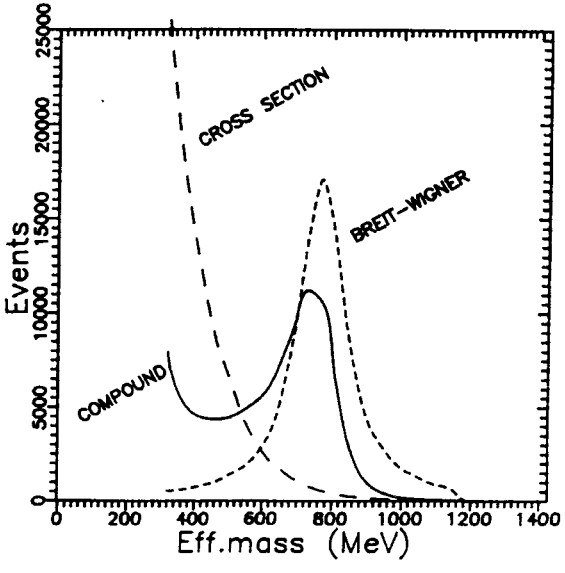

Fig.1. The two-pion effective mass distribution from the ρ meson decay for p_ρ = 500 MeV/c. The ρ meson production cross section mass dependence and Breit — Wigner mass distribution influence are plotted separately.

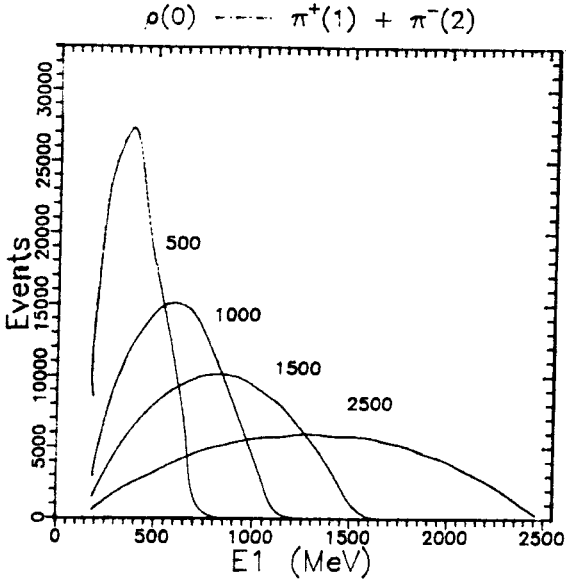

Fig.2. The one-pion energy distirubiton from the ρ meson decay for $p_0 = 500, 1000, 1500, 2500$ MeV/c.

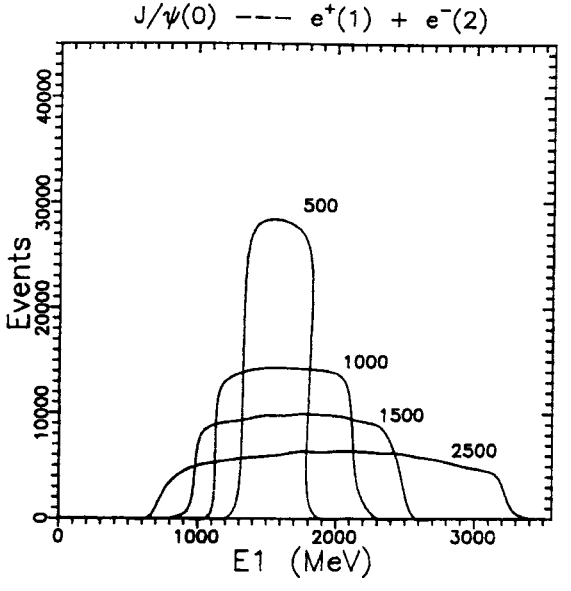

Fig.3. The one-electron energy distribution from the J/ψ meson decay for $p_{J/\psi} = 500$, 1000, 1500, 2500 MeV/c.

the ρ and J/ψ meson decay products are shown in Figs.2, 3. The dynamics (cross section) and Breit — Wigner affect the one-pion distribution from the ρ meson decay (Fig.2), modifying the pure kinematic to rectangular one. For the J/ψ decay, because the electron CM $\cos\theta_1^*$ has uniform distribution and the $\Gamma_{J/\psi} \approx 0$, the one-electron energy distribution in the laboratory system has also a uniform distribution, mainly a kinematic rectangular behaviour (Fig.3), between the limits:

$$E_1 = (E_1^* \cdot E_0 \pm |\vec{p}_1^*| \times$$

$$\times |\vec{p}_0| / m_0.$$

— The one-particle *angular distributions* for some meson momentum values are shown in Figs.4, 5. There can be seen a net particle flight, on the initial meson direction, especially evident for high momentum ρ meson. The J/ψ meson has a more flat angular distribution.

— The *opening angle distributions* of the two

particles from the ρ and J/ψ decay are presented in Figs.6, 7. For the two pions of the ρ meson decay, the opening angle distribution has a clear maximum for every ρ momentum values (Fig.6). For the two electrons of the J/ψ decay, the θ_{12} angle distribution shows a clear low limit, for every J/ψ energy value (Fig.7), in accordance with the well-known relation (when $m_1 = m_1 = m_2 \ll m_0$): $\theta_{12}^{\min} = -2 \arcsin (m_0/E_0)$.

— The last analyzed distribution is the one-particle *transverse momentum distribution* for the decay products of the ρ and J/ψ shown in Figs.8—11. Obviously, the distributions are very sensitive to the ρ and J/ψ meson emission angle θ_0. As long as $\theta_0 = 0°$, the one-particle transverse momentum distributions coincide for all the $\vec{p}_0$ values, while for $\theta_0 = 90°$ they show a strong momentum dependence (Figs.9,10). In the same time, the electron p_t distribution

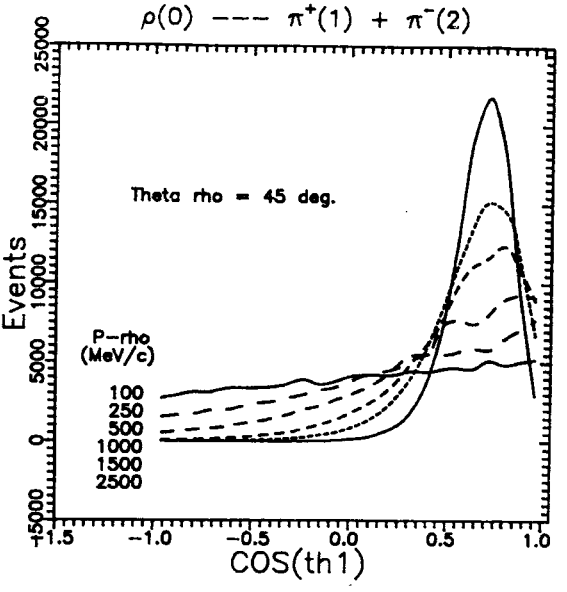

Fig.4. The one-pion angular distribution from the ρ meson decay, under $\theta_\rho = 45°$, for $p_\rho = 100$, 250, 500, 1000, 1500, 2500 MeV/c

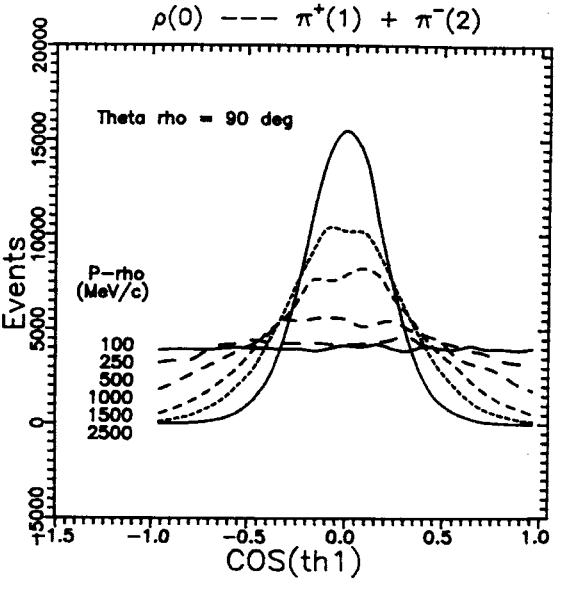

Fig.5. The one-pion angular distribution from the ρ meson decay, under $\theta_\rho = 90°$, for $p_\rho = 100$, 250, 500, 1000, 1500, 2500 MeV/c

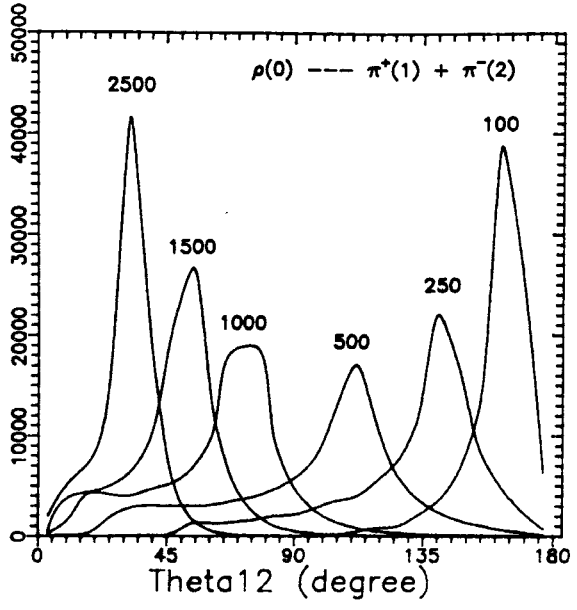

Fig.6. The relative flight angle distribution of the two pions from the ρ meson decay for p_ρ = 100, 250, 500, 1000, 1500, 2500 MeV/c

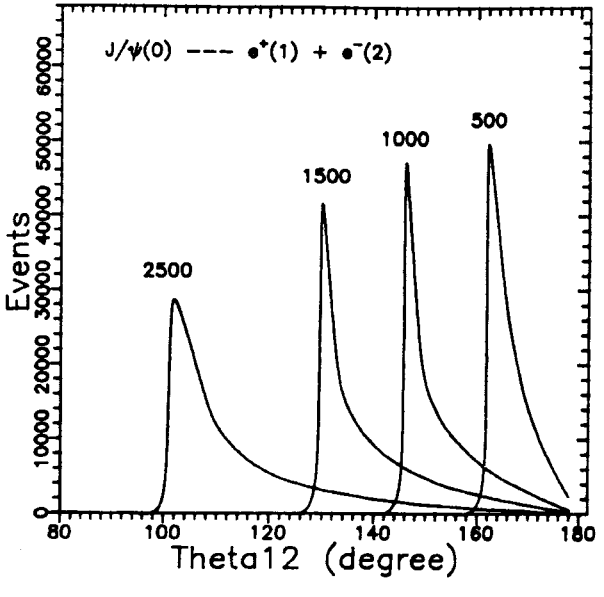

Fig.7. The relative flight angle distribution of the two electrons from the J/ψ meson decay for $p_{J/\psi}$ = 500, 1000, 1500, 2500 MeV/c

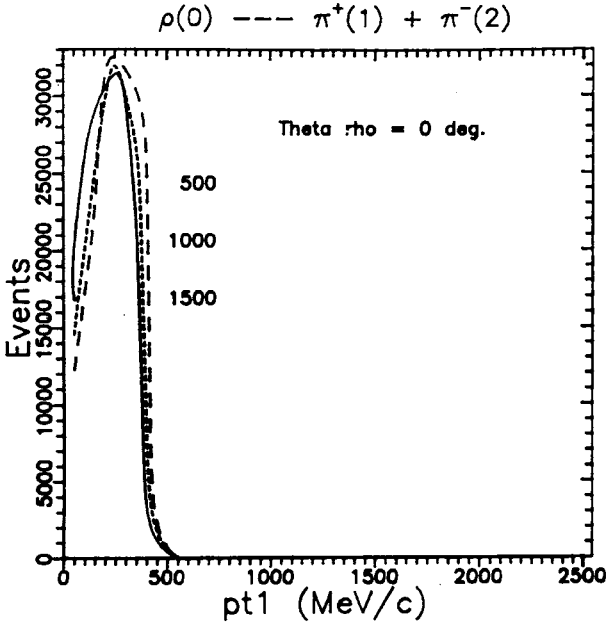

Fig.8. The one-pion transverse momentum distribution from the ρ meson decay, under $\theta_\rho = 0°$, for $p_\rho = 500$, 1000, 1500 MeV/c

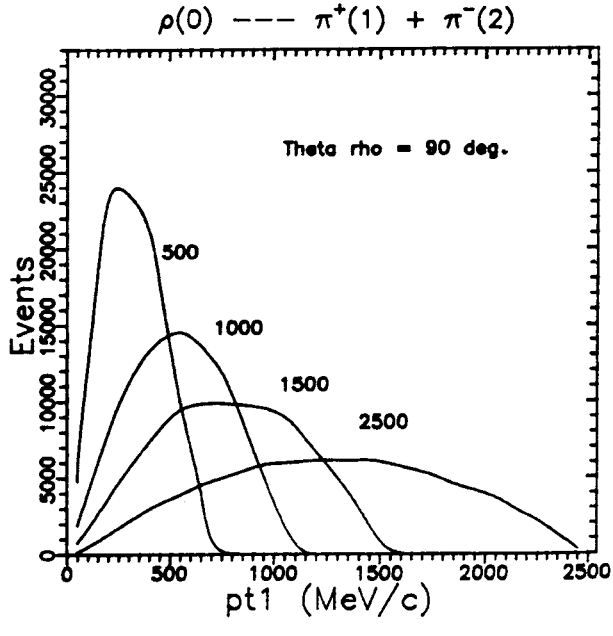

Fig.9. The one-pion transverse momentum distribution from the ρ meson decay, under $\theta_\rho = 90°$, for $p_\rho = 500$, 1000, 1500, 2500 MeV/c

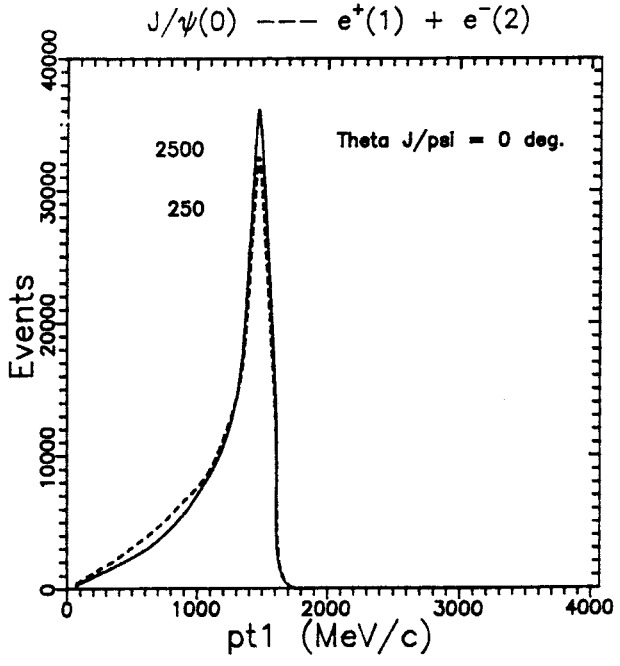

Fig.10. The one-electron transverse momentum distribution from the J/ψ meson decay, under $\theta_{J/\psi} = 0°$, for $p_{J/\varphi} = 250$, 2500 MeV/c

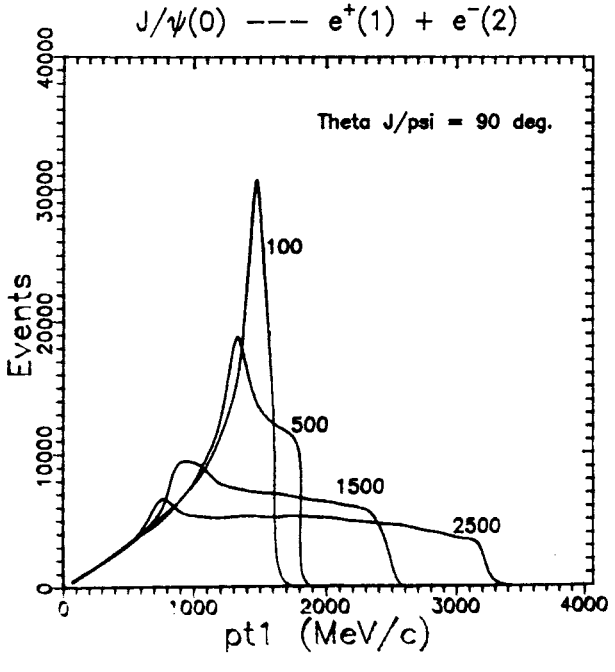

Fig.11. The one-electron transverse momentum distribution from the J/ψ meson decay, under $\theta_{J/\psi} = 90°$, for $p_{J/\psi} =$ 100, 500, 1500,

from the J/ψ decay for $\theta_0 = 0°$, shows a clear p_{t1}^{max} limit (Fig.10). If the cross section influence can be neglected, then the p_{t1}^{max} can be expressed, in the same $m_1 = m_2 << m_0$ approximation, as [10]: $p_{t1}^{max} = m_0/2$, and is independent of the J/ψ momentum (energy).

4. Conclusions

Phenomenological approach of the subthreshold production [6] was extended from the stable particle (pseudoscalar mesons, protons and antiprotons) to ρ and J/ψ vector meson production. Using the Monte — Carlo simulation and the final state phase space integration, we propose some particular distributions. Analyzing the characters, peculiarities and kinematical aspects of this distributions it is possible to prepare a proper experiment for the study of the ρ and J/ψ meson production in nuclear subthreshold interactions.

Acknowledgements. We wish to express special thanks to S.V.Afanasiev, V.V.Arkhipov, S.Reznikov and A.Yu.Semenov for computer assistance.

References

1. Baldin A.M. et al. — JINR, E1-8054, Dubna, 1974.
   Baldin A.M. et al. — JINR, E1-82-472, Dubna, 1982.
   Baldin A.M. et al. — JINR, P1-83-433, Dubna, 1983.
2. Gorenstein M.I., Zinovjev G.M. — Phys. Lett., 1977, 67B, p.100.
3. Berlad G., Dar A., Eilam G. — Phys. Rev. D, 1980, 27, p.1547.
4. Ghiordanescu N., Stavinsky V.S. — JINR, P2-81-369, Dubna, 1981.
5. Pentia M. et al. — St. Cerc. Fiz., t.37, N.6—8, p.740, Bucuresti, 1985, (in Romanian).
6. Stavinsky V.S. — Proceedings IX Int. Seminar on H.E.P.Problems, Relativistic Nucl. Phys. and Q.C.D., Dubna, 14—19 June, 1988, JINR D1,2-88-652, Dubna, 1988, p.190.
7. Halzen F., Martin A.D. — Quarks and Leptons, An Introductory Course in Modern Particle Physics, Wiley, New-York, 1984.
8. Kopylov G.I. — Osnovy Kinematiki Resonansov, Nauka, Moskva, 1970.
9. Sobolj I.M. — Chislennye Metody Monte-Carlo, Nauka, Moskva, 1973.
10. Goldansky V.I., Nikitin Yu.P., Rosental I.L. — Kinematicheskie Metody v Fizike Vysokikh Energij, Nauka, Moskva, 1987.

Received on July 7, 1992.